doi: 10.82124/CEAS-GNC-2026-016 CEAS-GNC-2026-016

EuroGNC Madrid, Spain May 5th-7th 2026

Midcourse Guidance Based on Augmented Pursuit Guidance for Ducted-Rocket Missiles

Min-Jea Tahk Professor Emeritus, Department of Aerospace Engineering, KAIST, 34141, Daejeon, Republic of Korea, mjtahk@kaist.ac.kr

Boseok Kim Ph. D. Student, Department of Aerospace Engineering, KAIST, 34141, Daejeon, Republic of Korea, kbobo6@kaist.ac.kr

Dain Jeong M. S. Student, Department of Aerospace Engineering, KAIST, 34141, Daejeon, Republic of Korea, dainj0124@kaist.ac.kr

Chang-Hun Lee Associate Professor, Department of Aerospace Engineering, KAIST, 34141, Daejeon, Republic of Korea, lckdgns@kaist.ac.kr

ABSTRACT

This paper proposes an Augmented Pursuit Guidance (APG)-based guidance law that faithfully tracks optimal trajectories by reproducing the optimal lead angle history with respect to the target. Although optimal guidance laws offer theoretical performance advantages, their real-time applicability is often limited due to computational complexity. To address this gap, the proposed APG method provides a practical and implementable alternative that closely approximates the optimal solution using precomputed or polynomial-approximated data. Simulation study shows that APG is a simple and efficient method for trajectory tracking during the mid-course guidance phase of a long-range air-to-air missile equipped with a dual-pulse rocket.

Keywords: Midcourse Guidance, Trajectory Following, Arrival Time Control, Pursuit Guidance

1 Introduction

Recently, air-breathing ducted rockets have been adopted as propulsion systems for long-range air-to-air missiles. Ducted rockets utilize incompletely combusted gas emitted from a gas generator within the rocket, which is then mixed with air entering the combustion chamber through the inlet before being expelled. Ducted rockets boast a specific impulse more than three times that of conventional solid-fuel rockets, enabling them to cruise for hundreds of kilometers. Furthermore, solid propellants can be filled in the combustion chamber to act as boosters during the initial launch phase. Solid-fuel rockets, such as dual-pulse rockets, require a maximum altitude of more than 30 km for long-range flight. However, if the target maneuvers to produce any PIP (predicted intercept point) change, the trajectory correction of the missile can be a challenging task to handle at high altitudes. Ducted rockets, on the other hand, are normally operated at altitudes lower than 20 km due to the air-breathing nature, making PIP changes much easier to handle.

To maximize the benefits of ducted rockets, proper trajectory shaping is more effective than constant-altitude cruising. In other words, real-time trajectory optimization can further increase the operational range. Convex programming, being widely studied for trajectory optimization, provides rapid solutions and is therefore an ideal tool for this optimization problem. However, because the missile/environment model used to calculate the optimal trajectory is not identical to reality, even the open-loop control input of the optimal trajectory cannot accurately track the optimal trajectory. One way to overcome these trajectory errors is to iterate real-time trajectory optimization every few seconds. However, unlike initial trajectory optimization, in-flight trajectory optimization also requires constraints on PIP arrival time. A variation in the PIP arrival time can lower the missile seeker's target acquisition success rate or significantly increase the maneuver acceleration required during the terminal homing guidance phase, potentially reducing the hit probability of the engagement.

Performing real-time trajectory optimization on the missile's onboard computer is simpler from an operational perspective than performing it on the launch aircraft and transmitting the optimal trajectory information to the missile. Although the launch-and-forget mode is preferable, repeatedly calculating optimal trajectories every few seconds on the missile computer inevitably imposes a significant computational burden and requires a high-performance on-board computer, which inevitably increases costs. A more practical alternative is to perform trajectory optimization on the launch aircraft before launch and once or twice after launch to update the PIP. In this operational scenario, the missile needs to independently control its trajectory and speed to reach the PIP at the arrival time specified by the optimal trajectory.

This paper proposes a midcourse guidance method that employs a predetermined optimal trajectory to accurately reach the predicted impact point (PIP) at a specified arrival time, even in the presence of errors in the initial conditions and vehicle dynamic models. Various techniques have previously been studied to follow a precomputed optimal trajectory. The perturbation guidance based on the linear quadratic regulator [1] follows the optimal trajectory by linearizing the missile dynamics at each time step and applying optimal feedback gains. While this approach provides a mathematically rigorous framework, its performance is highly dependent on frequent and accurate linearization. Polynomial fitting that approximates the optimal trajectory using time-dependent polynomial functions is a simple approach to generate guidance commands [2], but its performance can be highly sensitive to initial condition errors and temporal disturbances. Sliding mode control studied in [3] is an alternative, but high-frequency switching in control inputs can cause chattering, which can excite unmodeled dynamics. Model predictive control may be adopted to solve a constrained optimization problem over a finite future horizon to follow the optimal path [4]. Although this method effectively handles physical and operational constraints, it demands high computational power on board. It should be noted that none of these approaches has considered the problem of arrival time errors.

In this paper, the augmented pursuit guidance (APG) method [5] is adopted, and a new algorithm is introduced to regulate arrival time by controlling the flow rate of the ducted rocket gas generator. First, we briefly introduce the ducted-rocket mathematical model used in this study. This in-house model calculates thrust based on inlet airflow and the gas generator flow rate. The trajectory optimization method used to maximize the terminal velocity is also briefly described. Next, we analyze the miss-distance characteristics of APG to derive a closed-form solution for a simple scenario, and numerically investigate the effects of various error sources on the arrival time. Finally, we present an arrival-time control algorithm and provide simulation results to demonstrate that the proposed method enables the missile to reach the PIP at the specified time, despite the presence of multiple source of errors.

2 Trajectory Optimization of Ducted-Rocket Missiles

Variable-flow ducted rocket (VFDR) missiles utilize inhaled air as part of the oxidizer, resulting in higher propulsion efficiency than conventional solid rocket missiles. The structure of a ducted rocket missile can be simply described as follows: The gas generator combusts propellant to generate fuel-rich gas, which is then fed to the main combustor (secondary combustor) through a gas control valve. In the main combustion chamber this excess fuel gas mixes with inhaled air, resulting in secondary combustion and thrust generation. Based on the thrust generation principle described above, the thrust of a VFDR missile is affected by flight conditions such as the flight Mach number, altitude, air-fuel ratio, and angle of attack, expressed as follows:

$$T = T(M, h, \alpha, AF) \tag{1}$$

where the performance ratio AF is defined as the ratio of air intake and fuel consumption rate expressed as

$$AF = \frac{\dot{m}_a}{\dot{m}_f} = \frac{\rho(h)\ V\ I(\alpha)}{\dot{m}_f} \tag{2}$$

In the above equation, $I(\alpha)$ represents the effect of the angle of attack on the air intake. Due to the strong nonlinearity of the ducted rocket propulsion process, the thrust is not given in an analytical function form. Instead, it is constructed in the form of a data table for the decision variables, as described in [6]. The two-dimensional equations of motion on the vertical plane is the same as ordinary missile dynamics:

$$\begin{aligned}
\dot{x} &= V\cos\gamma, \\
\dot{h} &= V\sin\gamma, \\
\dot{V} &= \frac{-D + T\cos\alpha}{m} - g\sin\gamma, \\
\dot{\gamma} &= \frac{L + T\sin\alpha}{mV} - \frac{g\cos\gamma}{V}, \\
\dot{m} &= -\dot{m}_f
\end{aligned} \tag{3}$$

where D and L represent drag and lift, respectively, and g is acceleration due to gravity. Based on the geometry of the Meteor missile, drag and lift are calculated for each operating condition, and they are determined as functions of speed, altitude, and angle of attack, as follows:

$$L = L(V, h, \alpha), \quad D = D(V, h, \alpha) \tag{4}$$

In this study, thrust, lift, and drag, given in Eqs. (1) through (4), are modeled using artificial neural networks. Each artificial neural network consists of two hidden layers with five nodes. Ducted rocket missiles have the following flight constraints to ensure stable combustion of the propulsion system.

$$\alpha_{\min} \le \alpha \le \alpha_{\max}, \tag{5}$$

$$AF_{\min} \le AF \le AF_{\max}, \tag{6}$$

$$\dot{m}_{f,\min} \le \dot{m}_f \le \dot{m}_{f,\max} \tag{7}$$

In order to optimize the trajectory of the midcourse guidance phase, the state variable is selected as $z = [\ h,\ V,\ \gamma,\ m]^T$ and the control input is selected as $u = [\alpha, AF]^T$. Both two sides of the equation of motion given by (3) are divided by $\dot{x}$ to replace the independent variable t by the range x to obtain the following system equation:

$$\dot{z} = f(z, u) \tag{8}$$

The Legendre-Gauss-Radau (LGR) pseudospectral method [7] is then utilized for discretization to construct a trajectory optimization problem consisting of discrete variables. In this method, the domain of the independent variable is replaced from $x \in [x_0, x_f]$ to $\xi \in [-1, 1]$ through an affine transformation, and the discretized state variables and control input vectors are defined at the node locations $(\xi_1, \ldots, \xi_{N+1})$ that include both of the boundary nodes.

$$\begin{aligned}
\boldsymbol{Z} &= [Z_1, \ldots, Z_{N+1}]^T, \quad \text{where } Z_i = [h_i, V_i, \gamma_i, m_i]^T, \\
\boldsymbol{U} &= [U_1, \ldots, U_N]^T, \quad \text{where } U_i = [\alpha_i, AF_i]^T
\end{aligned} \tag{9}$$

Now the system equation of (3) can be expressed as the following relationship between the discretized state variables and control input vectors according to the LGR pseudospectral method:

$$\boldsymbol{D Z} = \frac{x_f - x_0}{2} \boldsymbol{F}(\boldsymbol{Z}, \boldsymbol{U}), \quad \text{where } \boldsymbol{F}(\boldsymbol{Z}, \boldsymbol{U}) = [f(Z_1, U_1), \ldots, f(Z_N, U_N)]^T \tag{10}$$

In the above formula, $\boldsymbol{D}$ is the Ladau differentiation matrix with a constant value. In the midcourse guidance phase, the objective is to reach the PIP with the maximum terminal speed from the initial launch condition by using the limited amount of the fuel. The problem is then written as a constrained parameter optimization problem as follows:

$$\min_{\boldsymbol{Z}, \boldsymbol{U}} \quad J = -V_{N+1} \tag{11}$$

subject to

$$\boldsymbol{Z}_0 = [\, h_0,\ V_0,\ \gamma_0,\ m_0 \,]^T, \tag{12}$$

$$h_{N+1} = h_f, \quad m_{N+1} \geq (m_0 - m_f), \tag{13}$$

$$\text{Eqs. (5), (6), (7) and (10).}$$

In this study, GPOPS-II has been utilized to obtain the optimal trajectory. However, real-time trajectory optimization requires a high-speed optimization solver such as sequential cone programming (SCP) [8], which can find the optimal trajectory in less than one second with the current desktop computer.

3 Augmented Pursuit Guidance for Trajectory Following

Augmented Pursuit Guidance (APG) has been studied for polynomial trajectory generation since it can quickly generate the guidance command from the polynomial coefficients [9–11]. Later, its usefulness for trajectory following was suggested, since the altitude of any trajectory can be approximated by a polynomial of the downrange [5]. For the implementation of the optimal trajectory of a long-range missile, APG is a powerful method for trajectory following, because its algorithm is very simple and the altitude-tracking error converges to a sufficiently small value even when the mathematical model used for trajectory optimization differs from the real world.

For the pitch channel, APG is expressed as

$$a_{\text{com}} = N\, V\, (\lambda_{\text{ref}} - \lambda) \tag{14}$$

where $a_{\text{com}}, N, V, \lambda_{\text{ref}}$, and λ represent the normal-acceleration command, guidance gain, missile speed, reference trajectory lead angle, and missile lead angle, respectively. The lead angle is defined as $\lambda = \gamma - \sigma$ where γ is the flight-path angle and σ is the line-of-sight (LOS) angle from the missile to the target position, as illustrated in Figure 1.

In this work, the reference trajectory is defined as the optimal trajectory approximated by a polynomial of an order lower than that of the polynomial order used for the trajectory optimization based on the pseudospectral method. Nonetheless, the terminal altitude of the polynomial trajectory is identical to that of the optimal trajectory as the coefficients of the polynomial trajectory are determined to satisfy this condition. The downrange to go, denoted as x_{go}, is chosen as the independent variable of the polynomial trajectory since it is more convenient than the downrange for the derivation of the lead angle. The details of the polynomial approximation are described in [5].

The APG method is very simple in structure since it calculates the normal acceleration command by feeding back the difference between the lead angle of the reference trajectory and that of the current

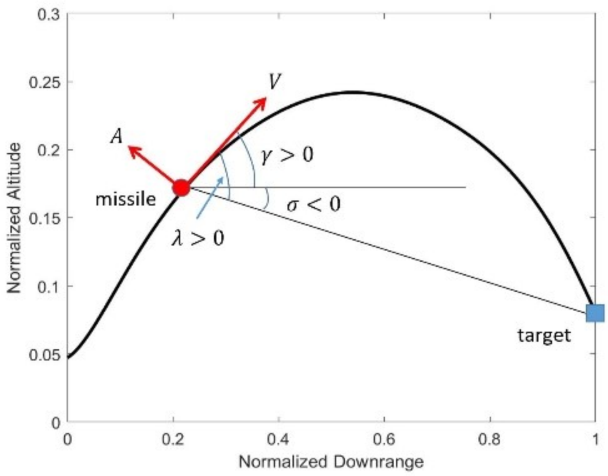

Fig. 1 Definitions of symbols

trajectory. Generally, the tracking error, defined as the altitude difference between the reference trajectory and the actual trajectory, decreases as the missile approaches the target, but it can temporarily increase if the flight path angle of the reference trajectory keeps changing. While it is easy to observe these characteristics through simulation, analytical results on the final altitude error for an arbitrary reference trajectory are hard to obtain. Therefore, this study considers the simplest scenario where the reference trajectory is a straight line connecting the launch point and the PIP located at the same altitude. Note that the lead angle of this reference trajectory, $\lambda_{ref}(t)$, is always 0. Then, the acceleration command is expressed as

$$a_{com} = NV(\sigma - \gamma) = NV\left[-\frac{h}{(x_f - x)} - \gamma\right] \tag{15}$$

where $\sigma = -h/(x_f - x)$ is used assuming that the missile's line of sight to PIP is small. By substituting $\dot{\gamma} = a_{com}/V$, $\gamma = dh/dx$, and $V = dx/dt$ into this equation, the following equation can be obtained.

$$\dot{\gamma} = \frac{d^2h}{dx^2}\frac{dx}{dt} = -N\left[\frac{h}{(x_f - x)} + \frac{dh}{dx}\right] \tag{16}$$

By defining the constant $k = N/V$, Eq. (16) can be rewritten as a second-order differential equation of h as

$$\frac{d^2h}{dx^2} + k\frac{dh}{dx} + \frac{k}{(x_f - x)}h = 0 \tag{17}$$

For simplification, we introduce a new variable $\xi = x_f - x$. Then, the new differentiation operator is $d/dx = -d/d\xi$. Applying this, Eq. (17) becomes

$$h''(\xi) - kh'(\xi) + \frac{k}{\xi}h(\xi) = 0 \tag{18}$$

Using the substitution $h(\xi) = \exp(k\xi/2)v(\xi)$, the first derivative term is eliminated and $v(\xi)$ satisfies the following equation:

$$v''(\xi) + \left(\frac{k}{\xi} - \frac{k^2}{4}\right)v(\xi) = 0 \tag{19}$$

Rewriting Eq. (19) using $z = k\xi$ gives

$$\frac{d^2v}{dz^2} + \left(\frac{1}{z} - \frac{1}{4}\right)v = 0 \tag{20}$$

The above equation is identified as a special form of the Whittaker equation [12]. Similar cases of confluent hypergeometric equations are found in the interpretation of the PN derivation law [13, 14]. The solution of Eq. (20) has singularity at the terminal time and can be expressed using the exponential integral function $\mathrm{Ei}(x)$ as follows:

$$h(t) = C_1(x_f - x) + C_2 \left[(x_f - x)\, \mathrm{Ei}(k(x_f - x)) - \frac{\exp(k(x_f - x))}{k} \right] \tag{21}$$

$$\gamma(t) = -[C_1 + C_2\, \mathrm{Ei}(k(x_f - x))] \tag{22}$$

Given the initial conditions $h(0) = h_0$ and $dh/dx(0) = \gamma_0$, the constants C_1 and C_2 are determined as

$$\begin{aligned} C_1 &= -\gamma_0 + k(h_0 + \gamma_0\, \xi_0) \exp(-k\, \xi_0)\, \mathrm{Ei}(k\xi_0), \\ C_2 &= -k(h_0 + \gamma_0\, \xi_0) \exp(-k\, \xi_0) \end{aligned} \tag{23}$$

From these results, we observe that the altitude error at the final time converges to

$$h(t_f) = (h_0 + \gamma_0\, \xi_0) \exp(-k\, \xi_0) \tag{24}$$

and the flight path angle response has a singularity at the final time. Eq. (24) shows that the terminal altitude error is the initial zero-effort miss (ZEM) exponentially attenuated over the flight time.

4 Effects of Model Uncertainties

The first simulation study is to investigate the effect of model uncertainties on the arrival time at PIP. It is assumed that the missile accelerates horizontally by burning the solid propellant filled in the ducted rocket's combustion chamber, reaching Mach 2 before igniting the ducted rocket. This simulation study considers the burn-out state of the boost phase as the initial condition of the midcourse guidance phase. The optimal trajectory is also computed only for the phase propelled by the ducted rocket. Trajectory optimization using GPOPS-II assumes a limited 27.2 kg of fuel to generate a trajectory that reaches the PIP at a range of 100 km at maximum speed. Three scenarios are considered, each with the same PIP range but different altitudes of 5, 10, and 15 km. The optimal trajectory data are given at 31 nodes and the optimal altitude history is approximated by a seventh-order polynomial of downrange, which is used as the reference trajectory to follow. In polynomial approximation, a preprocessing step is performed to normalize the altitude and range by the downrange of the PIP, denoted as X_f. Figures 2 and 3 show the results of tracking the optimal trajectory with APG in each scenario. The same dynamic model used for trajectory optimization is employed in this simulation.

Although the PIP altitudes are different, a common tendency is observed to slightly lower the missile's altitude initially. This is because higher air density improves the efficiency of the ducted rocket. In other words, descending to an altitude where the thrust increase is greater than the drag increase can maximize the terminal velocity while using the same propellant weight. In each figure, the trajectory generated by APG appears to accurately follow the optimal trajectory, but the altitude tracking error can be as much as 80 m depending on the PIP altitude, as shown in Figure 4. In this figure, the initial altitude error is not exactly 0 since the initial altitudes of the optimal trajectory and its polynomial approximation do not exactly match at the initial time.

In all three scenarios, the arrival time error is less than 0.1 s, and the terminal altitude error is within 3 m, as summarized in Table 1. In particular, the velocity error is within 3 m/s, indicating that the terminal velocity performance of the optimal trajectory is hardly degraded. Additionally, fuel consumption is reduced by approximately 0.02 kg due to the reduced terminal speed.

The following simulations analyzes the effects of various model errors and winds on the PIP arrival time, terminal altitude, and terminal velocity, for the PIP of 10 km altitude, and the results are summarized in Table 2. A 500 m error in the initial position results in a 0.5 second difference in the PIP arrival time, which is not significant. However, if the initial velocity is 30 m/s (approximately a 5% error) greater than the optimal trajectory, the PIP arrival time is shortened by 2.162 seconds and the terminal velocity increases by 3.89 m/s. A 5% error in thrust not only has a similar effect on the PIP arrival time but also has a significant effect on the terminal velocity. A 5% error in the drag coefficient is about half the effect of a 5% error in thrust. Contrary to expectations, a typhoon-level headwind does not have a significant effect. This is because the increased air speed of the missile due to the headwind increases engine thrust, partially compensating for the increased drag. The ducted rocket design used in this simulation has the advantage of being relatively insensitive to headwinds and tailwinds. However, the effects of crosswinds could be significant since the efficiency of a ducted rocket decreases with non-zero sideslip angles. Crosswind effects will be addressed in future research.

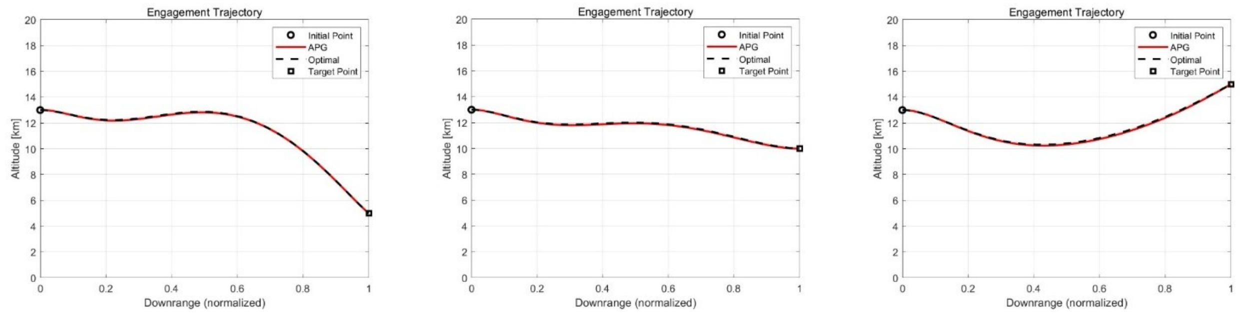

(a) H_{PIP} = 5 km (b) H_{PIP} = 10 km (c) H_{PIP} = 15 km

Fig. 2 Optimal trajectory followed by APG

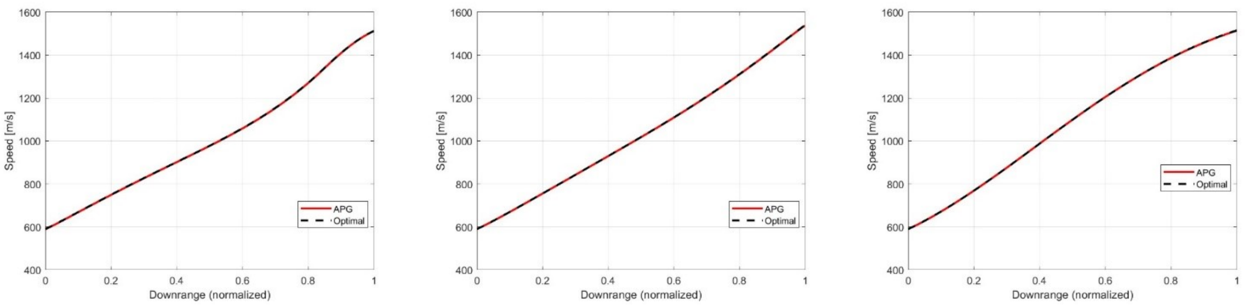

(a) H_{PIP} = 5 km (b) H_{PIP} = 10 km (c) H_{PIP} = 15 km

Fig. 3 Speed history produced by APG

Figure 5 shows the altitude tracking errors of APG under the presence of the initial speed error and the engine thrust error. It is clearly observed that the altitude tracking errors of APG are insensitive to the model errors. This result implies that the missile's travel distance under APG is almost invariant for given engagement scenario. Using this property, a simple algorithm can be employed for the control of the arrival time.

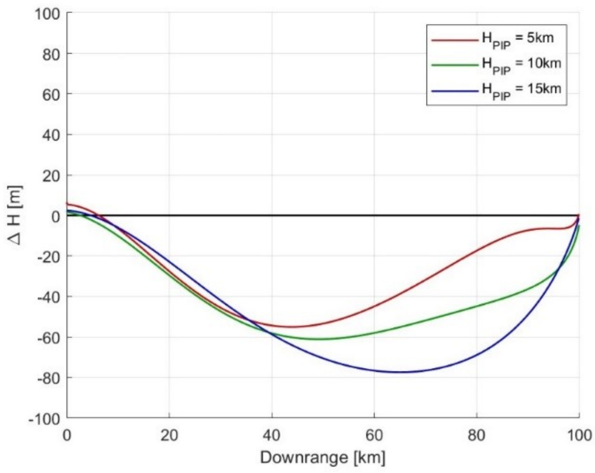

Fig. 4 Altitude tracking errors under model uncertainties.

Table 1 APG tracking errors at PIP

H_{PIP} (km)	Δt_f (s)	ΔH_f (m)	ΔV_f (m/s)	$\Delta\gamma_f$ (deg)	Δm_f (kg)
5	+0.063	-2.15	-0.59	+0.35	-0.022
10	+0.030	-1.96	-2.28	+1.31	-0.020
15	+0.047	-0.72	-0.97	+0.57	-0.021

Table 2 Effects of model errors and winds on the terminal states (H_{PIP} = 10 km)

Error Source	Δt_f (s)	ΔH_f (m)	ΔV_f (m/s)	$\Delta\gamma_f$ (deg)	Δm_f (kg)
ΔX_0 = +500 m	-0.523	-1.97	-3.33	+1.06	-0.073
ΔV_0 = +30 m/s	-2.162	-1.95	+3.89	+1.25	-0.407
ΔT = +5%	-1.885	-2.13	+40.58	+1.42	-0.578
ΔC_D = +5%	+0.840	-1.90	-21.10	+1.26	+0.219
head wind 25 m/s	+0.306	-2.08	-9.96	+0.98	+0.025
tail wind 25 m/s	-0.203	-2.02	+4.38	+0.99	-0.139

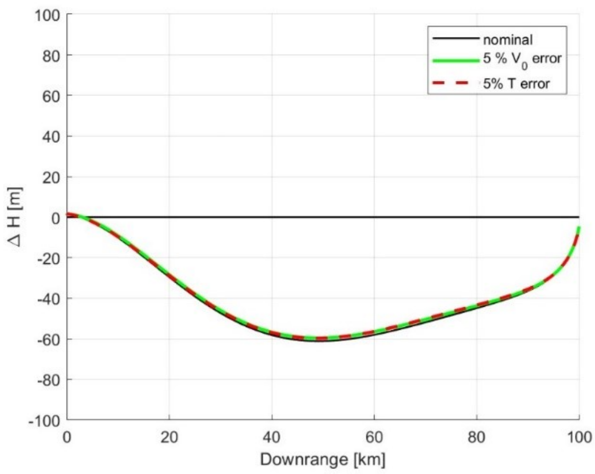

Fig. 5 Altitude tracking errors under model uncertainties

5 PIP Arrival Time Control

As discussed in the previous section, when modeling errors or initial-condition errors exist in the missile dynamics, APG generates a flight trajectory close to the optimal trajectory in the $(X,\ H)$ plane. The PIP arrival time, however, deviates from that of the optimal trajectory. To minimize the PIP arrival-time error, the following method is proposed. We define t^* as the time on the optimal trajectory corresponding to the current range. The total distance along the optimal path from the current downrange position to the PIP is equal to the travel distance along the optimal trajectory over the interval $\left(t^*, t_f\right)$. Therefore, if $t < t^*$, the missile has a larger time to go, denoted as t_{go}, to cover the same path and reach the PIP. In this case, the missile should maintain a lower speed to reach the PIP at the terminal time of the optimal trajectory. Note that the optimal time to go and the current time to go are expressed as

$$\int_C \frac{ds}{v^*(s)} = t_f - t^*, \tag{25}$$

$$\int_C \frac{ds}{v(s)} = t_f - t. \tag{26}$$

Now the question is how to select $v(s)$ to satisfy (26). A simple choice of $v(s)$ is to scale $v^*(s)$ up or down to satisfy (26). This strategy is expressed as

$$v(s) = \left(\frac{t_f - t^*}{t_f - t}\right) v^*(s) \tag{27}$$

It is emphasized that this strategy is possible only when the remaining trajectory is expected to be close to the optimal trajectory, which is true for APG. Note that the use of (27) may have a numerical problem as $t_{go} = t_f - t$ goes to 0. In this study, the choice of $v(s)$ is switched to $v(s) = v^*(s)$ when t_{go} decreases to a small value.

The structure of the speed controller based on (27) is shown in Figure 6. A proportional-integral (PI) controller is employed to compensate the effect of the model uncertainties. Table 3 summarizes the terminal state errors obtained by applying APG with the proposed speed control algorithm. To evaluate the performance of the proposed method, the speed controller is intentionally activated when the downrange increases to 20 km. The simulation results show that the arrival time is well controlled for all error sources considered in Table 2. The worst performance is observed for the case of an initial speed error of +30 m/s. In this case, the missile advances faster than the speed specified by the optimal trajectory, resulting in a situation where $t < t^*$ and $v_{com}(t)$ is commanded lower than $v^*(t)$. This explains why ΔV_f is negative for this case.

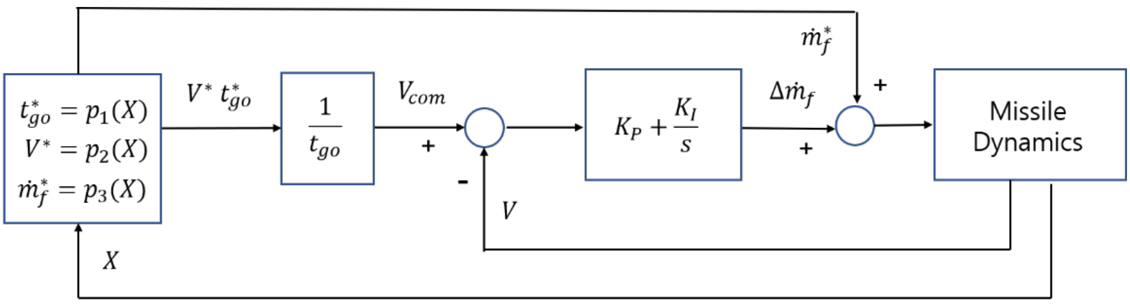

Fig. 6 Block diagram of the speed controller for arrival time control

Figure 7 compares the time-to-go histories for the cases of speed control ON and speed control OFF. If the time to go is positive at the PIP range, it indicates that the missile arrives at the PIP earlier than

Table 3 Terminal state errors with arrival time control (H_{PIP} = 10 km)

Error Source	Δt_f (s)	ΔH_f (m)	ΔV_f (m/s)	$\Delta \gamma_f$ (deg)	Δm_f (kg)
ΔV_0 = +30 m/s	+0.353	-1.90	-17.88	+1.27	-1.040
ΔT = +5%	+0.071	-1.96	+1.21	+1.31	-1.877
ΔC_D = +5%	+0.118	-2.00	-7.32	+1.39	+0.743
head wind 25 m/s	-0.003	-2.07	-1.19	+1.00	+0.339

the terminal time of the optimal trajectory. It is observed that an initial speed error produces noticeable time-to-go deviations from the beginning, whereas thrust and drag errors do not. The proposed arrival-time controller functions effectively under all model errors, but the plots suggest that it is preferable to activate speed control before the time-to-go errors grow to a significant level. Figure 8 illustrates the fuel flow rate histories for each model uncertainty. In this study, the tuning of the PI controller gains has been performed using these plots. Figure 9 presents the missile speed histories under the influence of model errors.

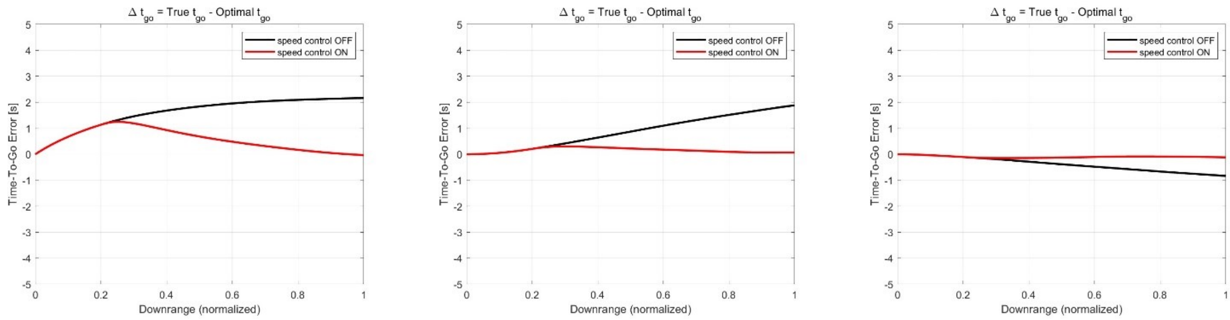

(a) ΔV_0 = +30 m/s (b) ΔT = +5% (c) ΔC_D = +5%

Fig. 7 Comparison of time-to-go history

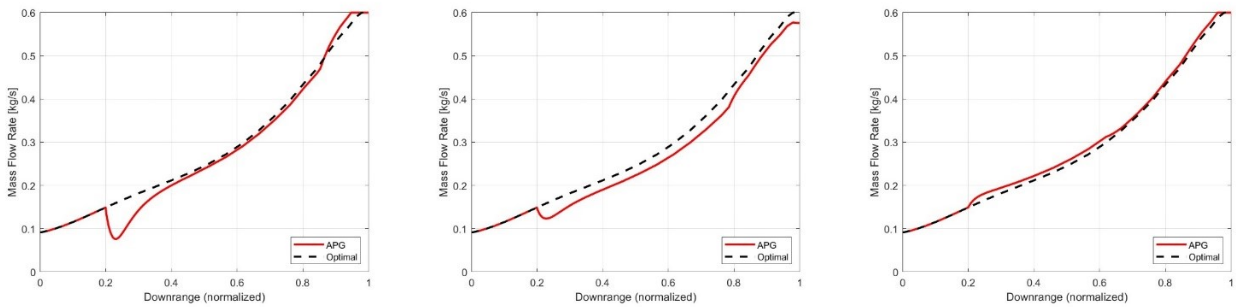

(a) ΔV_0 = +30 m/s (b) ΔT = +5% (c) ΔC_D = +5%

Fig. 8 Comparison of fuel-flow-rate history

6 Conclusions

This study proposes an arrival-time control method for long-range air-to-air missiles. The method leverages the small trajectory errors inherent in APG guidance to adjust the missile's speed such that it covers the remaining distance of the optimal trajectory within the remaining time to go. Simulation results demonstrate that the proposed method enables the missile to reach the PIP at the designated arrival time, even in the presence of large errors in initial speed, drag, thrust, headwind, or tailwind. Although not demonstrated here, the PIP arrival time can be flexibly adjusted during flight to accommodate

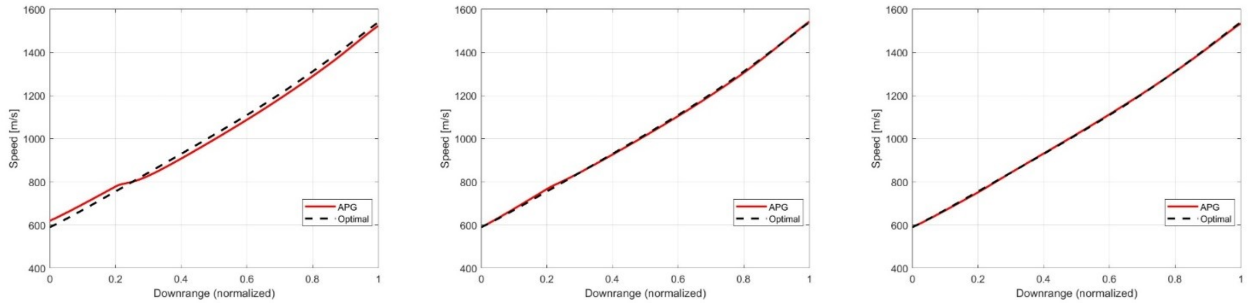

(a) ΔV_0 = +30 m/s (b) ΔT = +5% (c) ΔC_D = +5%

Fig. 9 Comparison of speed history

target velocity changes. For future research, a simulation code capable of handling three-dimensional engagement scenarios, together with a three-dimensional APG, will be developed to extend the speed-control algorithm to 3-D engagements. This will allow the proposed method to be validated against a broader range of dynamic model errors, such as crosswinds.

Acknowledgments

This work was supported by Theater Defense Research Center funded by Defense Acquisition Program Administration under Grant UD240002SD. The authors are very thankful for the technical comments of the project monitors of Agency for Defense Development.

Declaration of Use of Artificial Intelligence

The authors used ChatGPT (OpenAI, GPT-5, 2025 version) for language polishing only. The authors are fully responsible for the content and conclusions of this paper.

References

[1] P. Zarchan, *Tactical and Strategic Missile Guidance*, Progress in Astronautics and Aeronautics, AIAA, 2012.

[2] C. F. Lin, *Modern Missile Guidance*, CRC Press, 1991.

[3] Y. Shtessel et al., *Sliding Mode Control and Observation*, Springer, 2014.

[4] P. Falcone et al., "Predictive Control Approaches for Missile Guidance," Journal of Guidance, Control, and Dynamics, 2007.

[5] M. J. Tahk, B. Kim, O. Kang, and C. H. Lee, “Tracking Algorithms for Optimal Trajectories Based on Augmented Pursuit Guidance,” 11th European Conference for Aerospace Sciences (EUCASS), Rome, Italy, 2025.

[6] Y. K. Lee, H. G. Sung, and C. H. Lee, “Performance Analysis of a Ducted Rocket Under Various Flight Conditions,” International Journal of Aeronautical and Space Sciences, Vol. 26, No. 2, pp. 674-687, 2024.

[7] D. Garg, M. Patterson, W. W. Hager, A. V. Rao, D. A. Benson, and G. T. Huntington, “A Unified Framework for the Numerical Solution of Optimal Control Problems Using Pseudospectral Methods,” Automatica, Vol. 46, No. 11, pp. 1843-1851, 2010.

[8] B. Kim, and C. H. Lee, “Optimal Midcourse Guidance for Dual-pulse Rocket Using Pseudospectral Sequential Convex Programming,” Journal of Guidance, Control, and Dynamics, Vol. 46, No. 7, pp. 1425-1436, 2023.

[9] M. J. Tahk, J. C. Park, B. Kim, H. Roh, and C. H. Lee, "Augmented Pursuit Guidance for Flight Trajectory Shaping," Joint 10th EUCASS - 9th CEAS Conference, Lausanne, Switzerland, 2023.

[10] M. J. Tahk, J. C. Park, H. Roh, and C. H. Lee, "Suboptimal Guidance Based on Pursuit and Impact Angle Control for Long-Range Air-to-Air Missiles," 2023 14th International Conference on Mechanical and Aerospace Engineering, Porto, Portugal, 2023.

[11] M. Shin, M. J. Tahk, B. Kim, and C. H. Lee, "Pursuit-Based Long-Range Air-to-Air Missile Midcourse Guidance Robust to Changes in the Predicted Impact Point," 34th Congress of the International Council of the Aeronautical Sciences, Florence, Italy. 2024.

[12] F. W. J. Olver, A. B. Olde Daalhuis, D. W. Lozier, et al., "NIST Digital Library of Mathematical Functions," Release 1.2.1 of 2024-06-15, §13.14 Whittaker Functions, Available: https://dlmf.nist.gov/13.14

[13] T. Takehira, N. X. Vinh, P. T. Kabamba, "Analytical solution of missile terminal guidance," Journal of Guidance, Control, and Dynamics, Vol. 21, No. 2, March–April 1998.

[14] C. Markham, "Solutions of Linearized Proportional Navigation Equation for Missile with First-Order Lagged Dynamics," Journal of Guidance, Control, and Dynamics, Vol. 47, No. 3, March 2024.